Epitaxial growth of $CuGaSe_2$ thin-films by MBE – Influence of the Cu/Ga ratio

Andreas Popp[1] and Christian Pettenkofer[1]

[1]Helmholtz-Zentrum Berlin, Institute for Silicon Photovoltaics, Kekuléstraße 5, D-12489 Berlin, Germany

Corresponding author e-mail address: andreas.popp@helmholtz-berlin.de, Phone: +49 (0)30 8062-15697
E-mail address: pettenkofer@helmholtz-berlin.de, Phone: +49 (0)30 8062-15696

Abstract

By molecular beam epitaxy (MBE) $CuGaSe_2$ (CGS) thin-films with varying Cu/Ga ratios were grown epitaxial on GaAs (100) and stepped GaAs (111)A substrates. Cu/Ga ratios from Cu-poor to Cu-rich were obtained. In this work the appearance of Cu crystallites on the surface of epitaxial CGS (001) layers are observed and strategies to avoid these precipitations are presented. High quality thin CGS films of around 100 nm thickness are obtained, enabling a detailed analysis of the electronic and chemical properties as well as of the crystal structure of the CGS surfaces. The electronic structure with respect to the Cu/Ga ratio was characterized in-situ by XPS and UPS. By LEED a (4x1) (Cu-poor and near stoichiometric) and a (4x2) (Cu-rich) reconstruction of a zinc blende structure were obtained. For $CuGaSe_2$ (112) the LEED pattern showed a (3x1) chalcopyrite reconstruction for Cu/Ga ratios < 1. A (1x1) reconstruction of the chalcopyrite structure was observed for Cu-rich (112) samples. The observed dependence of the surface reconstruction on the stoichiometry for CGS grown on GaAs has not been reported in literature so far. Additionally, for Cu-rich stoichiometries a binary phase of $Cu_{2-x}Se$ appeared independently of orientation. The film morphology was investigated ex-situ by SEM.

Keywords compound semiconductor; chalcopyrites; $CuGaSe_2$; thin-films; MBE; LEED

1. Introduction

$CuGaSe_2$ (CGS) as an I-III-VI_2 compound semiconductor is part of the group of chalcopyrites. Because of the high absorption coefficient [1] and direct bandgap of 1.68 eV [2], CGS is a promising material for thin-film solar cell devices. A combination of the wide band gap chalcopyrite CGS with the low band gap $CuInSe_2$ in tandem devices promises cell efficiencies of around 25% [3,4]. To optimize the necessary heterostructures in a device, a profound understanding of the interface properties is essential.

This work focuses on the (001) and (112) surface preparation and in-situ characterization of single crystalline CGS thin-films. Epitaxial chalcopyrite thin-films can be prepared on GaAs and Si substrates by molecular beam epitaxy (MBE) [5–8]. A lattice mismatch of GaAs to CGS of 0.7% allows for a low defect density. For a dedicated investigation of electronic surface properties, a strict UHV environment for preparation and analysis was used.

2. Experimental

(100) and stepped (111)A orientated GaAs substrates were prepared. Previous studies on $CuInSe_2$ and $CuInS_2$ in our group lead to a well-established preparation procedure [8–10]. To provide a well-ordered, clean and oxide free surface, the substrate was degreased with ethanol and subsequently etched with a H_2O_2/NH_4OH and H_2SO_4/HCL solution for GaAs (100) and GaAs (111)A, respectively [11,12]. The substrate surface was protected against oxidation and dangling bond formation by a sulfur passivation with $(NH_4)_2S$. After transferring the sample to the integrated UHV system, an annealing step at 400°C for 30 minutes removed the sulfur passivation. The well-ordered substrate surface was checked in-situ by obtaining a (1x1) LEED pattern (Fig. 1).

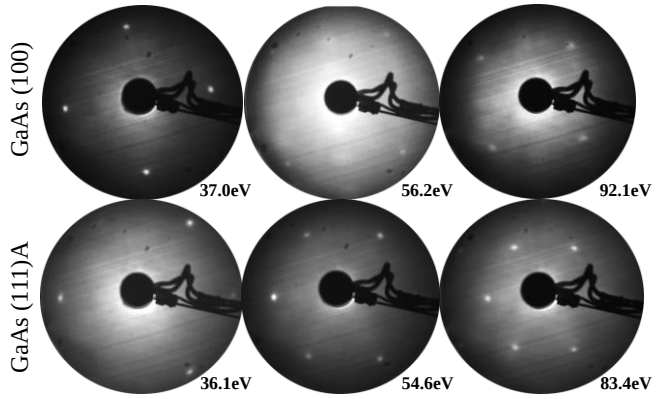

Fig. 1 LEED pattern of a GaAs (100) and GaAs (111)A substrate after a 30 min annealing step at 400°C.

Knudsen`s effusion cells for the elements Cu, Ga and Se were used. To change the Cu/Ga ratio, the Cu and Ga temperature were varied between 1080°C and 1160°C and 845°C and 900°C, respectively. Se was provided under excess conditions (T_{Se} = 200°C). Based on the phase diagram of CGS [13] the substrate temperature was set from 590°C to 600°C during growth. MBE chambers and analysis facilities are coupled by UHV transfers (integrated system) maintaining UHV conditions below $2 \cdot 10^{-10}$ mbar.

The epitaxial growth and crystal structure of the CGS thin-films were characterized by low energy electron diffraction (LEED) using an Omicron SpectraLEED. The electronic and chemical structure was analyzed with the focus on the Cu/Ga ratio by X-ray photo-electron spectroscopy (XPS) using a monochromatized Al K_α X-ray source (Specs Focus 500 monochromator) and a Specs Phoibos 150 analyzer equipped with a delay line detector. The valence band structure and the valence band maximum (VBM) were obtained by ultra-violet photo-electron spectroscopy (UPS), using a Helium discharge lamp. Ex-situ, the morphology was determined by scanning electron microscopy (SEM).

3. Results and Discussion

3.1 $CuGaSe_2$ (001)

In agreement with the CGS phase diagram [13], stoichiometries from Cu-poor to Cu-rich were achieved. The respective element concentration was determined by using the normalized intensity of the photo-emission peak measured by XPS weighted with element specific sensitive factors [14], which take into account the analyzer characteristic, the cross section of the photoionization and the mean free path of the photoelectrons [15]. The $Cu2p_{3/2}$, $Ga2p_{3/2}$ and Se3d emission lines were used to determine the molecularity (Cu/Ga) and the Se/(Cu+Ga) ratio. Cu/Ga ratios from 0.50 up to 1.70 were obtained by maintaining the Se/(Cu+Ga) ratio stoichiometric.

Except for the strongly Cu-rich sample all He I emission lines (Fig. 2) exhibit a chalcopyrite valence band structure, which is very similar to $CuInSe_2$ [8,16]. The VBM shifts towards the Fermi level for increased Cu/Ga ratios. This indicates a p-doping of the surface, as a Cu atom occupies a Ga site which leads to two additional positive charges.

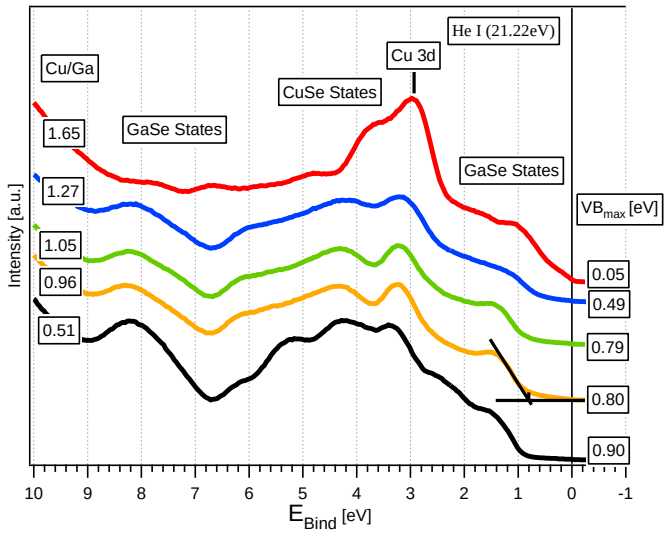

Fig. 2 He I data for $CuGaSe_2$ (001) samples with different stoichiometries measured by UPS.

For Cu-poor and near stoichiometric CGS layers a (4x1) single domain reconstruction of the zinc blende structure is obtained by LEED (Fig. 3) as known from literature for $CuGaSe_2$ (001) (for ex-situ prepared samples after suitable surface preparation) [17]. For Cu-rich samples a (4x2) reconstruction could be determined. Except for the near stoichiometric sample, the LEED spots are streaky with high background, which indicates an erratic stepped surface. Due to the GaAs substrate with its cubic structure, the CGS structure allows two rotation domains. However it seems that the larger parts of one domain may reorganize the whole surface to one domain, indicating a low formation energy for the (4x1) and (4x2) reconstruction.

Based on previous investigations on $CuInSe_2$ [8], the (4x2) structure was also expected for CGS. Deniozou et al. [18] explained this (4x2) structure as a termination with Se-dimers and Cu and In adatoms. For $CuInSe_2$ [19] this reconstruction appeared for all stoichiometries as single domain, regardless of the four fold symmetry of the substrate. For CGS in this series only Cu-rich layers showed a (4x2) reconstruction. If the Cu/Ga adatom order is missing, a (4x1) reconstruction is formed merely. This adatom order (4x2) seems to be more difficult to obtain for $CuGaSe_2$ than for $CuInSe_2$.

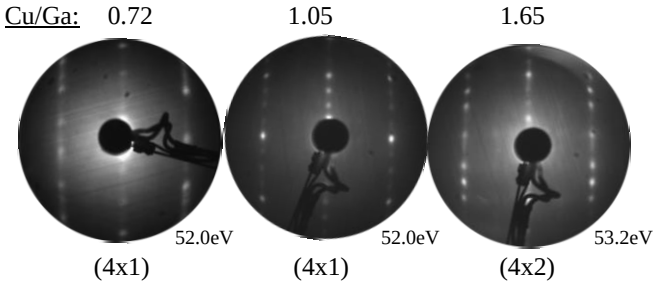

Fig. 3 LEED images of the $CuGaSe_2$ (001) surface for three different stoichiometry regimes. The different orientations of the LEED pattern are due to the sample mounting.

In Fig. 4 the XPS data of the $Cu2p_{3/2}$ peak with the corresponding Auger emission is depicted for different stoichiometries. A strong shoulder in the Cu core level as well as in the Auger line appears for all Cu/Ga ratios but becomes more pronounced for high Cu concentrations.

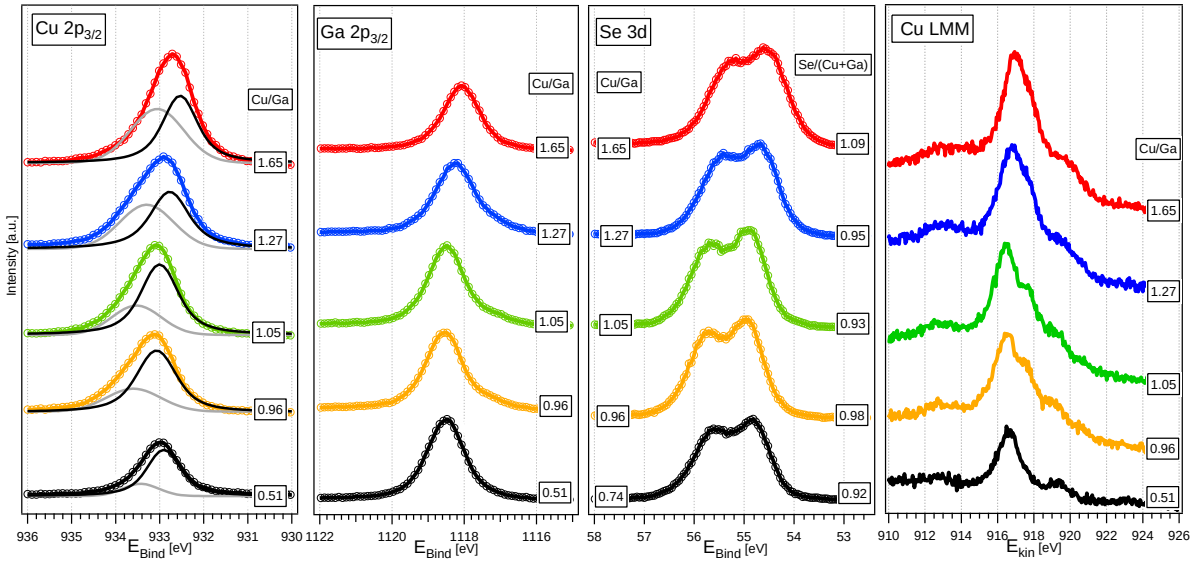

Fig. 4 XPS core level spectra and corresponding Cu Auger emission lines of $CuGaSe_2$ (001) samples for different stoichiometry regimes.

A line analysis of the $Cu2p_{3/2}$ peak (Fig. 5) for a Cu-rich sample, with a Cu/Ga ratio of 1.27, demonstrates that the Cu peak consists of at least two parts. In addition to the main component at 932.7 eV binding energy, a shoulder component at 933.3 eV is visible, which hints to a secondary phase on the surface.

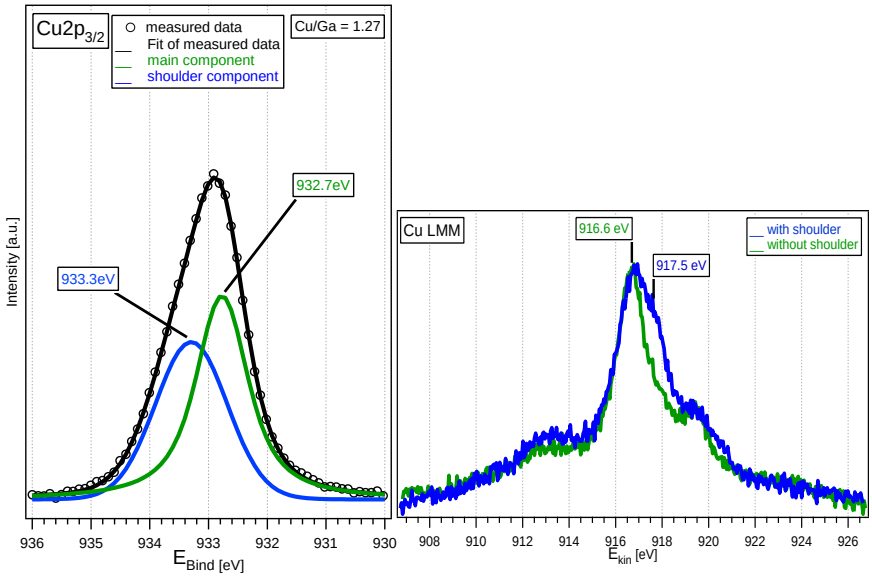

Fig. 5 $Cu2p_{3/2}$ XPS emission line with corresponding Cu LMM Auger emission line for a Cu-rich (Cu/Ga = 1.27) CGS (001) sample. The green Auger line is a reference measurement without a shoulder.

For the Auger line (Fig. 5 right) the shoulder component is located 0.9 eV above the main peak, at a kinetic energy of 917.5 eV. Difference spectra of the normalized Auger emission for high and low Cu concentrations were used to identify the shoulder position. A detailed investigation of the chemical environment can be obtained for the Cu Auger parameter α_{Cu} (eq. 1) [20]. This parameter combines the binding energy of the core level ($Cu2p_{3/2}$) with the kinetic energy of the corresponding Auger line (Cu $L_3M_{45}M_{45}$) [20]. In this way the determination of the chemical environment is independent of band bending shifts and doping effects as these contributions cancel out.

$$\alpha_{Cu} = E_{Bind}(Cu2p_{3/2}) + E_{kin}(CuL_3M_{45}M_{45}) \qquad (1)$$

If only considering the main components of the core level and the Auger line, α_{Cu} amounts to 1849.3 eV ± 0.2 eV. According to the NIST X-ray photoelectron spectroscopy database [21], this value is assigned to Cu-chalcopyrites. Taking into account the shoulder components solely, α_{Cu} changes to 1850.8 eV ± 0.2 eV. This indicates the presence of a binary phase of $Cu_{2-x}Se$ on the surface. A secondary phase of CuSe for Cu-rich copper chalcopyrites is already known [8,22–25].

Ex-situ characterizations of the surface morphology by SEM (Fig. 6) displays closed surfaces, which are partially covered with crystallites independent of the stoichiometry. These crystallites seem to form on the surface with no connection to the GaAs substrate and have grown simultaneously with the CGS epi layer.

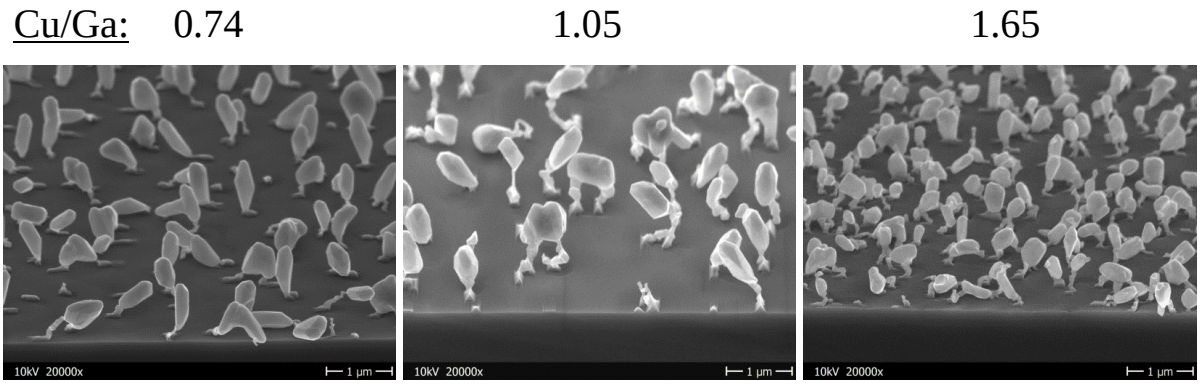

Fig. 6 SEM images of the $CuGaSe_2$ (001) surface for three different stoichiometry regimes.

With an extension of around 1µm, the precipitations can be analyzed by EDX which has an information depth of around 1000 nm [26]. The EDX investigation (Fig. 7) confirmed that the crystallites content of metallic copper (label A).

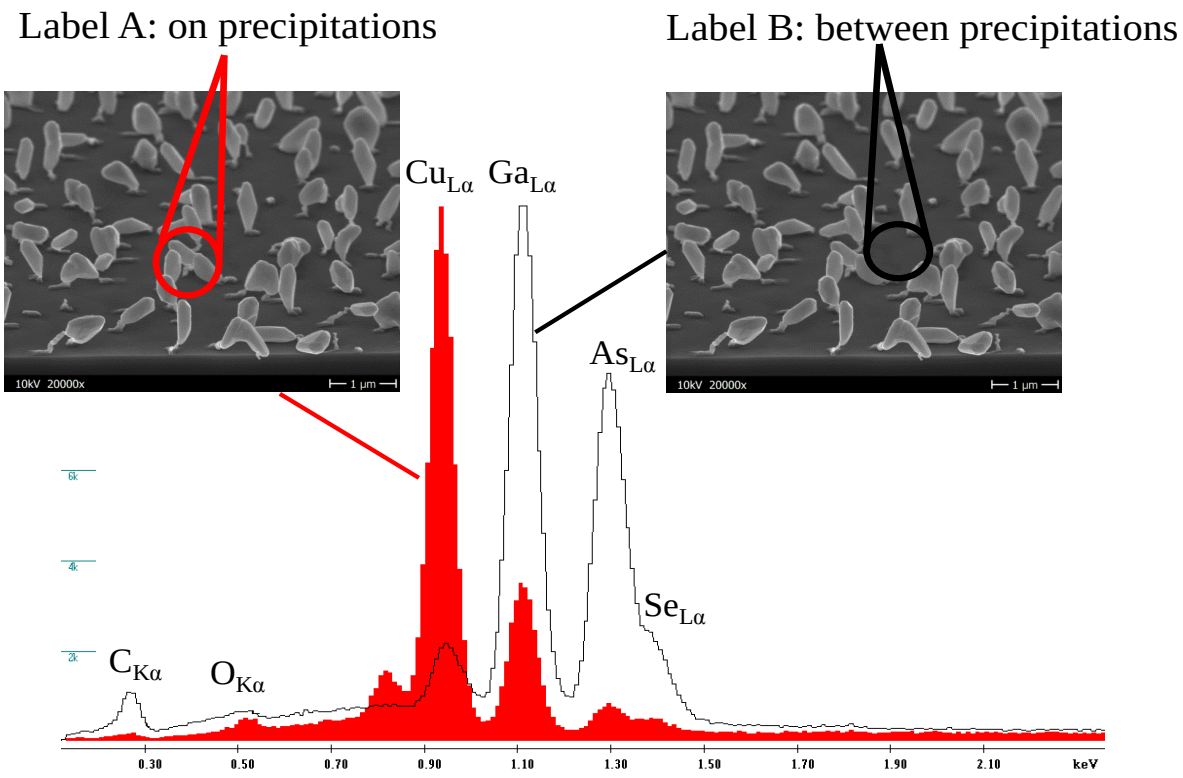

Fig. 7 EDX analysis of the precipitations on a CGS (001) layer.

The high Se pressure in the MBE chamber during the growth process is leading to a selenization of the surface of the copper crystallites and causes the appearance of a binary CuSe phase in the XPS spectra. Due to the high

surface sensitivity of the XPS, a signal of metallic copper with XPS is not expected. The CGS layer thickness is in the range of 50 nm – 100 nm hence the EDX spectrum between the precipitations is dominated by Ga and As from the GaAs substrate besides the $CuGaSe_2$ epitaxial top layer (label B). Different carbon contents (0.28 keV) result from the electron microscopy and are deposited by the e-beam in the SEM (no carbon is seen in the XPS data). To determining the stoichiometry by XPS the concentration of the specific elements are integrated over an array of the samples which includes parts with pure metallic Cu (on precipitations) and parts with lower Cu content (between precipitations). Due to the formation of these Cu precipitations, the calculated stoichiometry of the sample surface is flawed. Too much Cu is provided which segregates at the surface in Cu crystallites which are selenized at their surface contributing to a $Cu_{2-x}Se$ phase in the XP-spectra. For reducing the copper concentration the vapor pressures of the metal sources was adapted. As a consequence, the Cu cell temperature was decreased to 1070°C – 1080°C while the Ga cell temperature was increased to 935°C by maintaining the Se cell parameters. Using these adjusted growth parameters, it was possible to obtain $CuGaSe_2$ layers with stoichiometries from Cu-poor (Cu/Ga= 0.69) to Cu-rich (Cu/Ga = 1.58). Fig. 8 shows the XPS data of the $Cu2p_{3/2}$ core level and the corresponding Auger lines for different stoichiometries. Compared to Fig. 4 the shoulder has almost disappeared in the core level spectra as well as in the Auger lines. Only for Cu-rich Cu/Ga ratios a small shoulder at higher energies is observed.

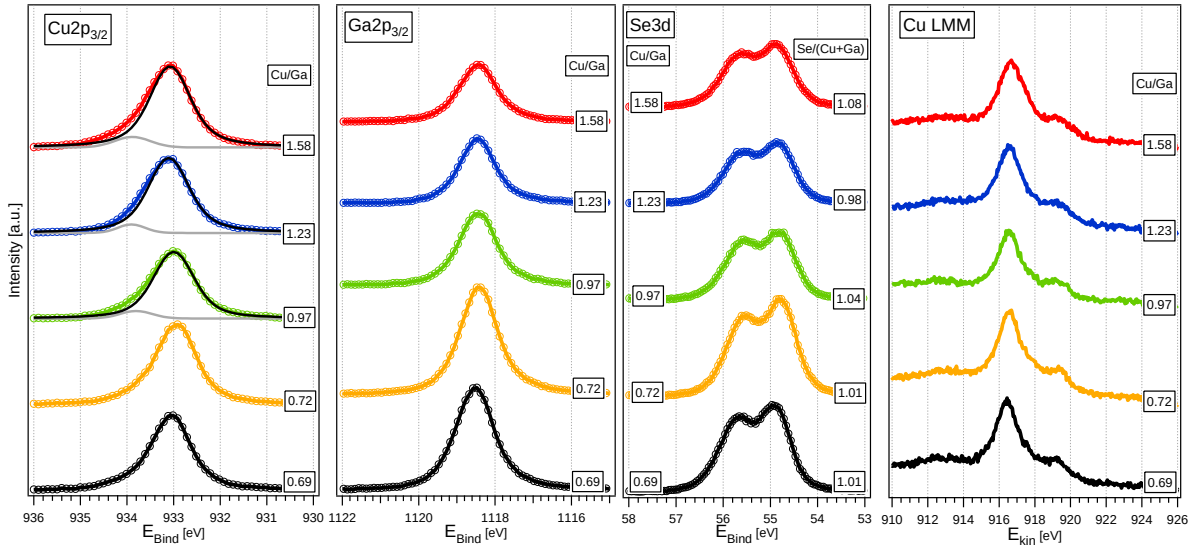

Fig. 8 XPS core level spectra and corresponding Cu Auger emission lines of $CuGaSe_2$ (001) samples (without Cu crystallites) for different stoichiometry regimes.

A direct comparison of the Auger lines (Fig. 9) of samples with and without Cu crystallites and the disappeared shoulder in the XPS data show that the metallic Cu component is removed.

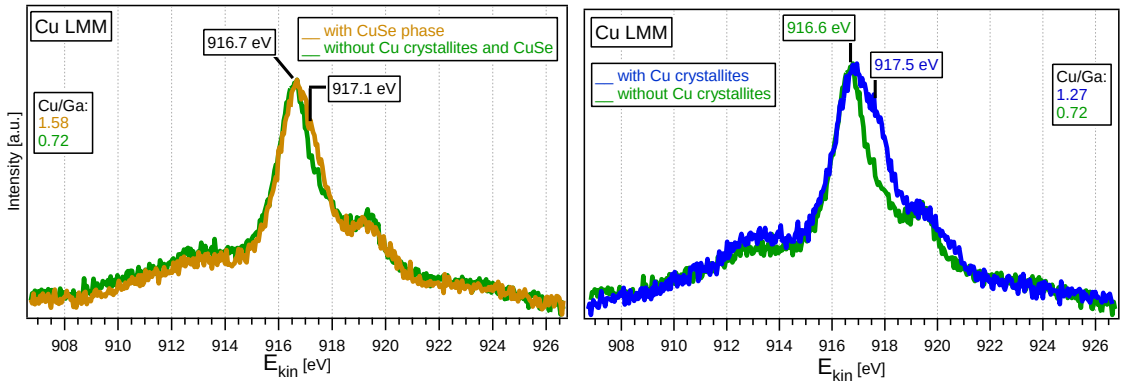

Fig. 9 Comparison of Auger emission lines for CGS (001) with (orange for CuSe and blue for Cu) and without (green) Cu crystallites.

A slight widening of the peak is visible for Cu-rich Cu contents only. By using the Cu Augerparameter α_{Cu} this could be assigned to a binary phase of $Cu_{2-x}Se$ phase, as expected for Cu-rich stoichiometries. Likewise, the determination of the kinetic energy of the shoulder component in the auger emission was carried out using difference spectra.

Except for very Cu-rich samples all valence band spectra depicted in Fig. 10, measured by UPS, exhibit a chalcopyrite structure. As already seen for the CGS samples with Cu precipitations (Fig. 2) the VBM shifts towards the fermi level by increasing the Cu/Ga ratio, which again hints to an increasing p-doping of the surface. The appearance of a CuSe binary phase for Cu-rich preparation conditions becomes also visible in the UP-spectra. For Cu/Ga ratios > 1 the valence band edge blurred out due to the overlapping valence band edges of the CGS and CuSe.

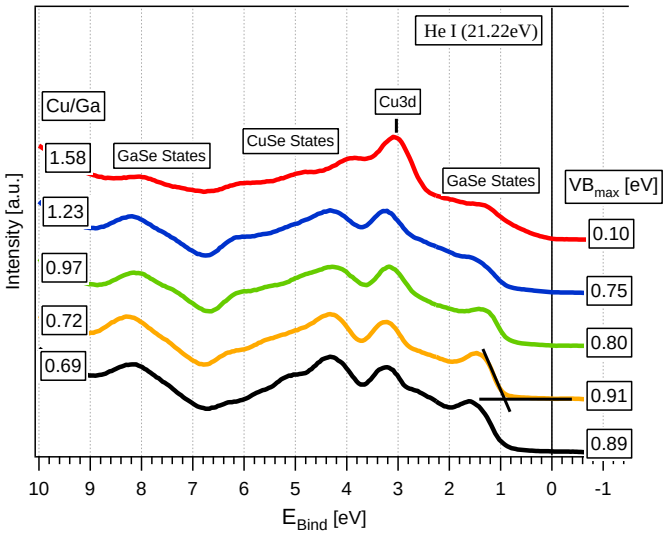

Fig. 10 He I data for $CuGaSe_2$ (001) samples (without Cu precipitations) with different stoichiometries measured by UPS.

After adjusting the vapor pressure of the metal element sources LEED images (Fig. 11) of the samples' surfaces show a clear and sharp (4x1) reconstruction of the zinc blende structure for Cu-poor and near stoichiometric CGS films.

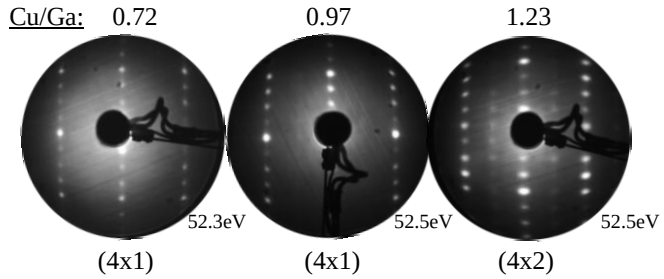

Fig. 11 LEED images of the $CuGaSe_2$ (001) surface for three different stoichiometry regimes [27].

For Cu-rich Cu/Ga ratios a clear (4x2) reconstruction is obtained. All images have low background intensity and streak free spots in common, indicating a high material quality and a low step concentration of the surface. As the (4x2) reconstruction is visible in the surface sensitive LEED pattern, a $Cu_{2-x}Se$ binary phase for Cu-rich layers cannot exist as a closed layer.

The growth of an epitaxial and flat CGS film surface is verified by an ex-situ investigation with SEM (Fig. 12). Brightness modulations maybe indicating for $Cu_{2-x}Se$ islands. Without Cu crystallites on the surface (Fig. 12a), a layer thickness of around 100 nm was obtained by analyzing the cross section (Fig. 12b).

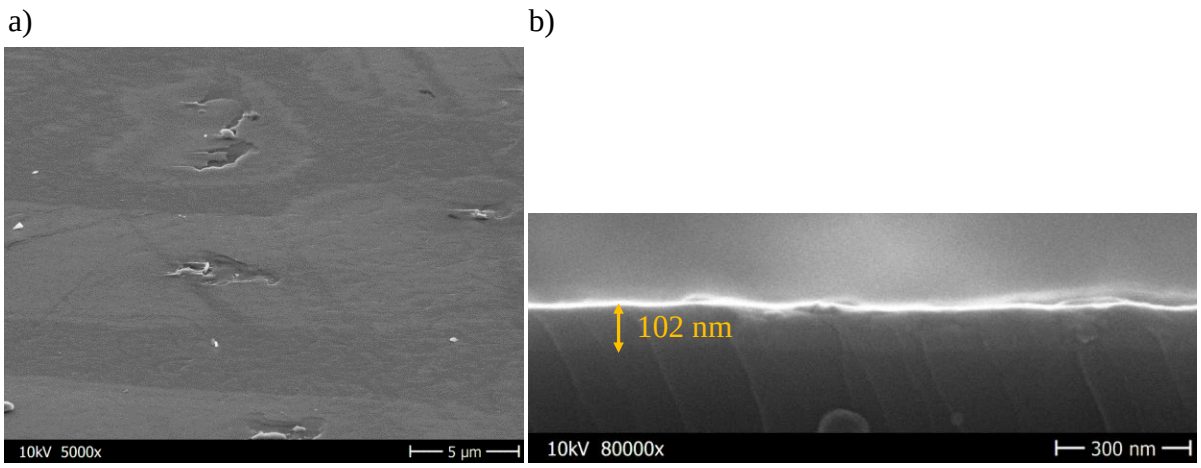

Fig. 12 SEM image of a near stoichiometric (Cu/Ga = 1.05) CGS (001) layer: a) top view tilted by 30°, b) cross section of the breaking edge [27].

3.2 $CuGaSe_2$ (112)

After establishing the growth procedure for $CuGaSe_2$ (001) on GaAs (100), $CuGaSe_2$ (112) films on GaAs (111)A were grown.

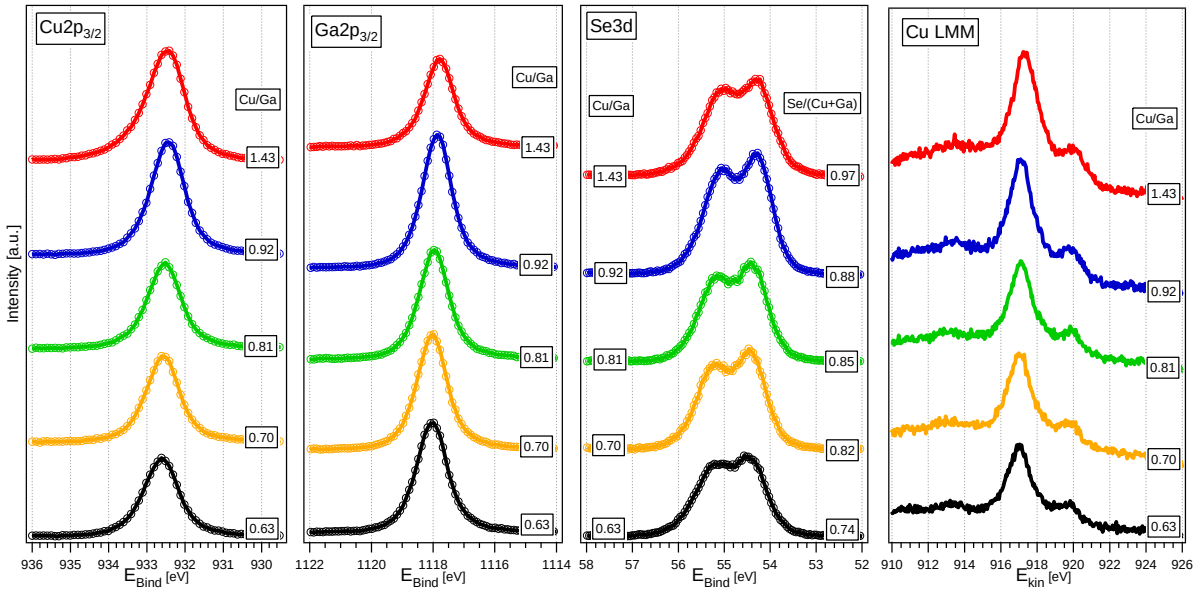

Fig. 13 XPS core level spectra and corresponding Cu Auger emission lines $CuGaSe_2$ (112) samples for different stoichiometry regimes.

The [112] direction is the natural growth direction of chalcopyrites in technologically prepared chalcopyrite films [28]. A stepped (111)A substrate with 5° miscut in [100] direction was used to suppress a growth of independent domains by step flow growth [8]. It was possible to prepare samples with stoichiometries from Cu-poor to Cu-rich with Cu/Ga ratios of 0.63 to 1.43 with (112) orientation with fixed stoichiometric Se/(Cu+Ga) ratio. Fig. 13 depicts the $Cu2p_{3/2}$ photoemission lines and the corresponding Auger lines. Independent of the stoichiometry, no pronounced shoulder can be observed. Just as for Cu-rich $CuGaSe_2$ (001) samples, a small shoulder in the Cu $2p_{3/2}$ emission line is visible for the sample with Cu/Ga = 1.43. Fitting the $Cu2p_{3/2}$ peak (Fig. 14) of a Cu-rich sample (Cu/Ga = 1.43), verifies that the Cu peak may consist of two parts. The main component can be located at 932.5 eV binding energy and the shoulder component at 933.3 eV. This indicates a secondary phase on the surface. By using difference spectra of the Auger line with and without a $Cu_{2-x}Se$ binary phase, it was possible to locate the shoulder component of the Cu LMM Auger line at 917.1eV kinetic energy. For Cu-

poor and near-stoichiometric samples α_{Cu} stayed in a range of 1849.5 eV to 1849.6 eV. For Cu-rich samples α_{Cu} increases up to 1850.8 eV ± 0.2 eV. Thus, the chemical environment of copper has changed for Cu-rich preparation conditions - a small amount of a $Cu_{2-x}Se$ phase is present at the surface.

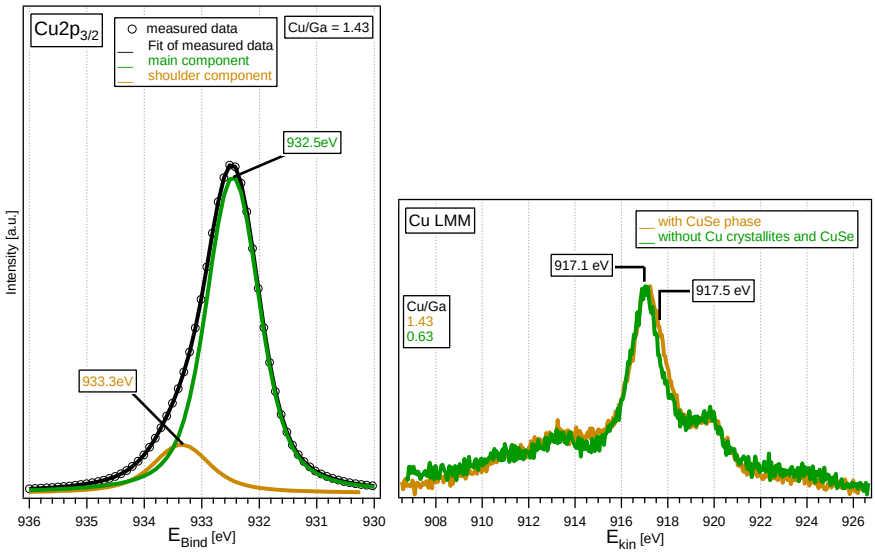

Fig. 14 $Cu2p_{3/2}$ XPS emission line with corresponding Cu LMM Auger emission line for a Cu-rich (Cu/Ga = 1.43) CGS (112) sample. The green Auger line represents a reference measurement without a shoulder (without $Cu_{2-x}Se$).

The secondary phase on the surface for Cu-rich samples can also be observed in the UP-He I spectrum. Fig. 15 compares the valance band spectra of $CuGaSe_2$ (112) samples with stoichiometries from Ga-rich to Cu-rich.

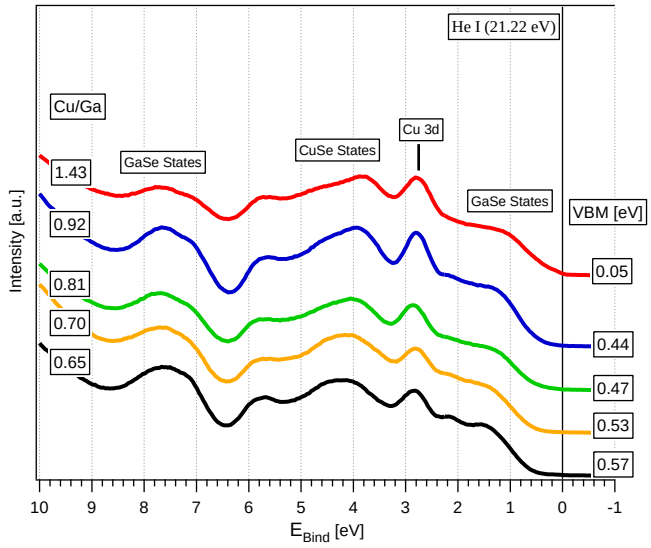

Fig. 15 He I spectra of $CuGaSe_2$ (112) layers for different stoichiometries.

The valance band edge is blurred out by increasing Cu-content. In agreement with the investigations of $CuGaSe_2$ (001) samples, the VBM shifts towards the Fermi level by increasing Cu/Ga ratios for $CuGaSe_2$ (112) samples. The surface doping changed from weakly n-conducting for Cu-poor samples to p-conducting for Cu-rich samples. Furthermore, the Cu3d peak increases slightly with the Cu/Ga-ratio.

For the [112] direction the LEED pattern (Fig. 16) exhibit the expected pattern for chalcopyrites consisting of the 3-fold symmetry from zinc-blende with the additional spots belonging to the chalcopyrite ordering (4x2) for all stoichiometries [8].

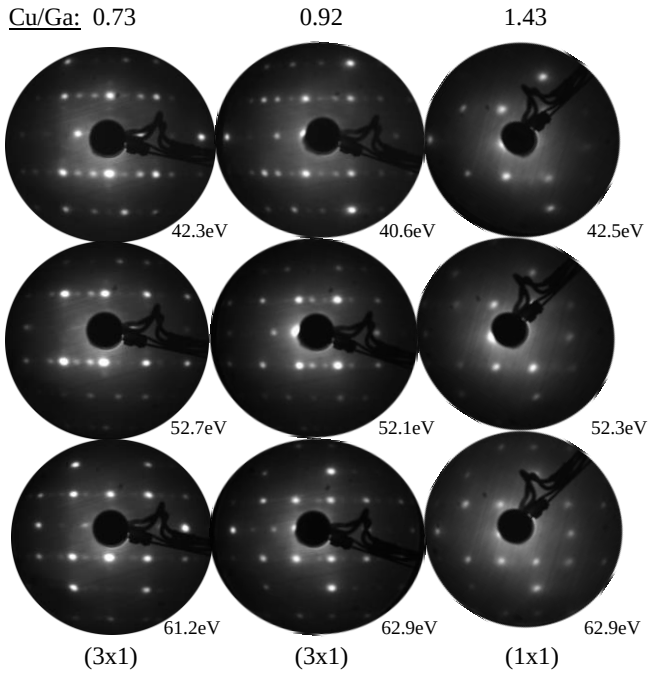

Fig. 16 LEED pattern of the $CuGaSe_2$ (112) samples grown on a stepped GaAs (111)A substrate for three different stoichiometry regimes.

A (3x1) single domain reconstruction for Cu-poor and near-stoichiometric conditions and a (1x1) reconstruction of the chalcopyrite structure for Cu-rich samples is observed. A Ga ordering in the Cu poor samples may be the reason for the (3x1) superstructure. Furthermore, the spots are sharper for Cu/Ga < 1 and the background is less intense, which indicates a higher quality of the layers.

An ex-situ investigation by SEM demonstrates that a flat epitaxial surface without Cu crystallites is formed (Fig. 17a). The analysis of the cross section (Fig. 17b) leads to the determination of the layer thickness to approximately 130 nm which gives a deposition rate of about 2 nm/min.

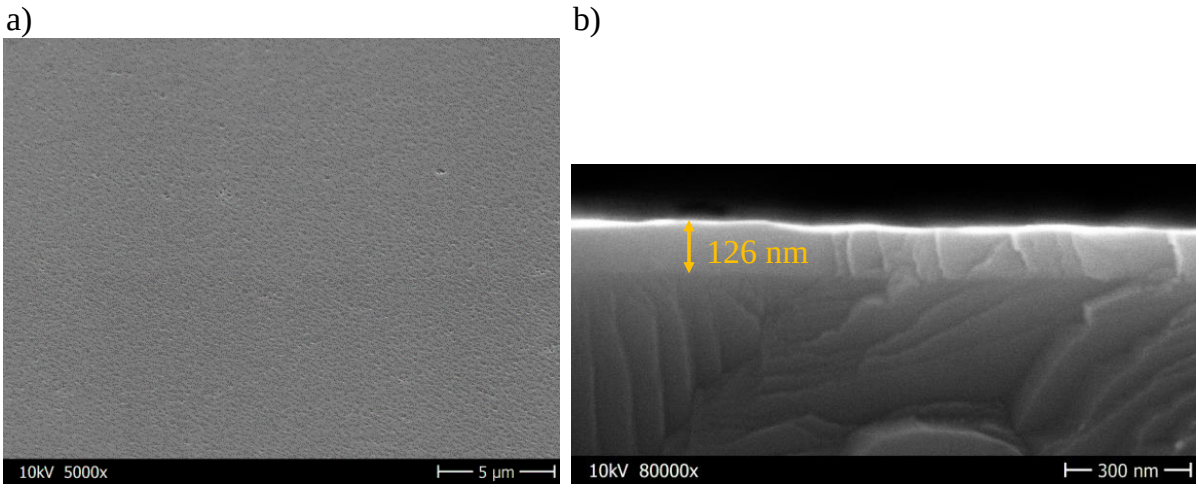

Fig. 17 SEM images of a near stoichiometric (Cu/Ga = 0.92) $CuGaSe_2$ (112) sample: a) top view tilted by 30°, b) cross section of the breaking edge.

4. Conclusion

Epitaxial $CuGaSe_2$ films were grown on GaAs (100) and stepped GaAs (111)A substrates by MBE. A presence of crystalline Cu precipitations was observed by SEM for CGS (001) layers. The formation of these Cu crystallites could be avoided by adjusting the vapor pressure of the copper and gallium sources. Well-ordered surfaces were detected by LEED. Thereby, a dependence of the surface reconstruction on the film stoichiometry was found. For the [001] direction a (4x1) reconstruction of the zinc blende structure for Cu-poor and near stoichiometric films transformed to a (4x2) reconstruction for Cu-rich samples. The $CuGaSe_2$ (112) samples exhibited a (3x1) single domain reconstruction of the chalcopyrite structure. For Cu-rich samples a (1x1) reconstruction was observed. According to the phase diagram of CGS, a $Cu_{2-x}Se$ binary phase was obtained by XPS for Cu-rich preparation conditions.

Acknowledgements

The authors gratefully acknowledge technical support by W. Bremsteller and H. Sehnert and a valuable discussion with G. Köppel.

References

[1] M. Belhadj, A. Tadjer, B. Abbar, Z. Bousahla, B. Bouhafs, H. Aourag, Structural, electronic and optical calculations of Cu(In,Ga)Se2 ternary chalcopyrites, Phys. Status Solidi Basic Res. 241 (2004) 2516–2528. doi:10.1002/pssb.200302045.

[2] R. Würz, M. Rusu, T. Schedel-Niedrig, M.C. Lux-steiner, H. Bluhm, M. Hävecker, E. Kleimenov, A. Knop-Gerike, R. Schögel, In-situ X-ray photoelectron spectroscopy study of the oxidation of CuGaSe2, Surf. Sci. 580 (2005) 80–94. doi:10.1016/j.susc.2005.01.054.

[3] M. Elbar, S. Tobbeche, A. Merazga, Effect of top-cell CGS thickness on the performance of CGS/CIGS tandem solar cell, Sol. Energy. 122 (2015) 104–112. doi:10.1016/j.solener.2015.08.029.

[4] M. Elbar, S. Tobbeche, Numerical Simulation of CGS/CIGS Single and Tandem Thin-film Solar Cells using the Silvaco-Atlas Software, Energy Procedia. 74 (2015) 1220–1227. doi:10.1016/j.egypro.2015.07.766.

[5] B. Schumann, C. Georgi, A. Tempel, G. Kühn, Epitaxial layers of CuInSe2 on GaAs, Thin Solid Films. 52 (1978) 45–52.

[6] T. Hahn, H. Metzner, B. Plikat, M. Seibt, Epitaxial growth of CuInS2 on sulphur terminated Si(001), Appl. Phys. Lett. 72 (1998) 2733–2735. doi:10.1063/1.121074.

[7] W. Calvet, C. Lehmann, T. Plake, C. Pettenkofer, Epitaxial CuInS2 on Si(111) using di-tert-butyl disulfide as sulphur precursor, Thin Solid Films. 480–481 (2005) 347–351. doi:10.1016/j.tsf.2004.11.090.

[8] A. Hofmann, C. Pettenkofer, Stoichiometry and surface reconstruction of epitaxial CuInSe2(112) films, Surf. Sci. 606 (2012) 1180–1186. doi:10.1016/j.susc.2012.03.017.

[9] A. Hofmann, C. Pettenkofer, The CuInSe 2-CuIn 3Se 5 defect compound interface: Electronic structure and band alignment, Appl. Phys. Lett. 101 (2012) 0–4. doi:10.1063/1.4739790.

[10] W. Calvet, H.J. Lewerenz, C. Pettenkofer, Model experiments on growth modes and interface electronics of CuInS2: Ultrathin epitaxial films on GaAs(100) substrates, Phys. Status Solidi Appl. Mater. Sci. 211 (2014) 1981–1990. doi:10.1002/pssa.201330429.

[11] K. Ueno, T. Shimada, K. Saiki, A. Koma, Heteroepitaxial growth of layered transition metal dichalcogenides on sulfur terminated GaAs {111}, Appl. Phys. Lett. 56 (1990) 327. doi:10.1063/1.102817.

[12] K.S.A. Butcher, R.J. Egan, T.L. Tansley, D. Alexiev, Sulfur contamination of (100) GaAs resulting from sample preparation procedures and atmospheric exposure procedures and atmospheric exposure, J. Vac. Sci. Technol. B. 14 (1996) 152. doi:10.1116/1.589018.

[13] P. Villars, H. Okamoto, eds., Cu-Ga-Se Vertical Section of Ternary Phase Diagram: Datasheet from "LINUS PAULING FILE Multinaries Edition – 2012" in SpringerMaterials (http://materials.springer.com/isp/phase-diagram/docs/c_0926514), (n.d.). http://materials.springer.com/isp/phase-diagram/docs/c_0926514.

[14] Specs, Quantification in XPS using SpecsLab and CasaXPS, (2008) 1–57.

[15] C.D. Wagner, L.E. Davis, M. V Zeller, J. a Taylor, R.H. Raymond, L.H. Gale, Empirical atomic sensitivity factors for quantitative analysis by electron spectroscopy for chemical analysis, Surf. Interface Anal. 3 (1981) 211–225. doi:10.1002/sia.740030506.

[16] A. Hofmann, C. Pettenkofer, Electronic band structure of epitaxial CuInSe_{2} films, Phys. Rev. B. 84 (2011) 1–8. doi:10.1103/PhysRevB.84.115109.

[17] T. Deniozou, N. Esser, S. Siebentritt, The CuGaSe2(0 0 1) surface: A (4 × 1) reconstruction, Surf. Sci. 579 (2005) 100–106. doi:10.1016/j.susc.2005.02.001.

[18] T. Deniozou, N. Esser, T. Schulmeyer, R. Hunger, A (4×2) reconstruction of CuInSe[sub 2] (001) studied by low-energy electron diffraction and soft x-ray photoemission spectroscopy, Appl. Phys. Lett. 88 (2006) 52102. doi:10.1063/1.2162677.

[19] A. Hofmann, Elektronische Struktur epitaktischer Chalkopyrite und deren Heterokontakte für die Photovoltaik, Dissertation, Brandenburgische Technische Universität Cottbus (BTU), 2012.

[20] J.F. Moulder, W.F. Stickle, P.E. Sobol, K.D. Bomben, Handbook of X-ray Photoelectron Spectroscopy, (1995) 255. doi:10.1002/sia.740030412.

[21] NIST X-ray Photoelectron Spectroscopy Database, (2012). https://srdata.nist.gov/xps/Default.aspx (accessed February 5, 2017).

[22] M. Fujita, A. Kawaharazuka, Y. Horikoshi, Characteristics of CuGaSe2 layers grown on GaAs substrates, J. Cryst. Growth. 378 (2013) 154–157. doi:10.1016/j.jcrysgro.2012.12.171.

[23] A. Yamada, Y. Makita, S. Niki, A. Obara, P. Fons, Growth of CuGaSe2 film by molecular beam epitaxy, Microelectronics J. 27 (1996) 53–58.

[24] S. Yoon, S. Kim, V. Craciun, W.K. Kim, R. Kaczynski, R. Acher, T.J. Anderson, O.D. Crisalle, S.S. Li, Effect of a Cu-Se secondary phase on the epitaxial growth of CuInSe 2 on (1 0 0) GaAs, J. Cryst. Growth. 281 (2005) 209–219. doi:10.1016/j.jcrysgro.2005.03.043.

[25] P. Fons, S. Niki, A. Yamada, H. Oyanagi, Direct observation of the Cu2-xSe phase of Cu-rich epitaxial CuInSe2 grown on GaAs (001), J. Appl. Phys. 84 (1998) 6926. doi:10.1063/1.368991.

[26] M. Henzler, W. Göpel, Oberflächenphysik des Festkörpers, 2. Auflage, B. G. Teubner Stuttgart, 1994.

[27] A. Popp, C. Pettenkofer, Epitaxial Thin Films of CuGaSe 2 Prepared on GaAs (001) Electronic Structure and Morphology, Ieee Pvsc. (2016) 2–6. doi:10.1109/PVSC.2016.7749640.

[28] Z.A. Shukri, C.H. Champness, Cleavage and Twinning in CuInSe 2 Crystals, Acta Crystallogr. Sect. B Struct. Sci. 53 (1997) 620–630. doi:10.1107/S0108768197004539.